This article has been accepted for publication in IEEE Access. This is the author's version which has not been fully edited and content may change prior to final publication. Citation information: DOI 10.1109/ACCESS.2023.3336706

IEEE Access
Multidisciplinary | Rapid Review | Open Access Journal

Research on the impact of indoor control quality monitoring based on Internet of Things

Lidong Pang[1], Chunyong Luo [1], Weidong Pan [2*]
Department of Civil Engineering, School of Architectural Engineering, Jinggangshan University, Ji'an 343009, China
Department of Mechanical Engineering, School of Mechanical and Electrical Engineering, Jinggangshan University, Ji'an 343009, China

***Abstract*—In recent years, indoor air quality monitoring has been a major concern worldwide due to its significant impacts on human health as people typically spend approximately 90% of their time in indoor environments. Many studies are increasingly focusing efforts on the design of real-time indoor air quality monitoring systems using wireless sensor networks. This paper presents a real-time cost-effective indoor air quality monitoring system (IAQMS) based on LoRa and the Internet of Things (IoT), which can measure CO_2, PM2.5, PM10, TVOC, HCHO, ambient temperature, and relative humidity. The hardware architecture and software design of the indoor air quality detector (IAQD) are described in detail. Based on the OneNET platform, the proposed IAQMS enables remote monitoring and storage of data in the cloud platform for future analysis. The measurement consistency and stability of the IAQD proposed in this study are verified through the experimental measurement methods in five different working conditions. Meantime, the effect of adding a shell on the measurement of the sensor is comparatively analyzed. The presented IAQMS can be flexibly deployed in complex indoor environments for real-time monitoring and alerting.**

***Index Terms*—Indoor air quality monitoring, Internet of Things (IoT), Sensors, LoRa, Outer Shell**

1. Introduction

The air pollution poses a huge challenge to global health. According to a survey by the WHO (World Health Organization), approximately 90% of the world's population breathes polluted air, causing 7 million deaths annually [1]. Many studies have focused on outdoor air pollution and its adverse effects on human health [2,3]. However, indoor air pollution is no less harmful than outdoor air quality pollution, as humans spend nearly 90% of their time indoors, such as in offices, schools, homes, and shopping malls [4,5]. The U.S. Environmental Protection Agency lists poor air quality as one of the five major environmental risks that endanger public health because indoor pollutant levels may be 100 times higher than outdoor pollutant levels [6]. Indoor air quality (IAQ) is affected by several parameters such as temperature, relative humidity, CO, CO_2, formaldehyde (HCHO), total volatile organic compound (TVOC) and particulate matter (PM2.5, PM10) [7,8]. Poor IAQ will develop health issues and lead to a set of symptoms, including headaches, dizziness, difficulties in concentration, and others, referred to as "sick building syndrome" (SBS) [8,9], which will seriously affect human health and work efficiency [10,11]. Therefore, a real-time indoor air quality monitoring system (IAQMS) is required, which can collect data from different locations and make it universally available, so that interested users can get IAQ information from the place they choose or plan.

Twenty years ago, some researchers needed to use a bag to evaluate IAQ, which is called an "air bag". The air was sampled and then brought back to the laboratory for analysis [12-14]. At that stage, most of the air quality detectors were relatively huge and complicated to operate, so it was difficult to achieve real-time on-site detection. With the rapid development of sensor technology and electronic technology, portable IAQ data collectors, called dataloggers, began to appear in the next period, which can be placed in a suitable location at the test site for field measurement. After the experiment, the data can be exported to a computer for data analysis through an SD card or USB communication [15-18]. Nowadays, wireless sensor network (WSN) technology and Internet of Things (IoT) technology make data collection and transmission more convenient. As long as there is network access, the monitored parameters can be accessed through the Web or mobile APP anytime and anywhere [19-24]. Compared with "air bag" or "datalogger", the IoT-based indoor air quality monitoring system allows for the monitoring of spatially varying phenomena, such as the IAQ in buildings [25].

Since environmental parameters are not unique, attention needs to be paid to environmental monitoring parameters. On the one hand, researchers focus on IAQ through single-sensor monitoring [22, 25-28]. A single parameter cannot bring good monitoring effects and reflect environmental conditions. On the other hand, research on sensor technology for monitoring IAQ has made great progress in the past ten years [29-33]. Many types of sensors can be applied to indoor environment monitoring systems.

* Corresponding author.
E-mail address: 9920050062@jgsu.edu.cn.

This work is licensed under a Creative Commons Attribution-NonCommercial-NoDerivatives 4.0 License. For more information, see https://creativecommons.org/licenses/by-nc-nd/4.0/

This article has been accepted for publication in IEEE Access. This is the author's version which has not been fully edited and
content may change prior to final publication. Citation information: DOI 10.1109/ACCESS.2023.3336706

In this study, a real-time and efficient indoor air quality monitoring system based on LoRa and IoT is proposed. The main contributions of this article are as follows.

1) A prototype IAQD is designed and developed based on LoRa, which monitors the temperature, relative humidity, CO_2, PM2.5, PM10, TVOC, and HCHO.
2) A real-time IAQMS is presented. The system is deployed with four IAQDs through experiments in an office of Jinggangshan University. The system has also developed a mobile APP display GUI, which can report the air quality data to users in real-time, and has an alarm push function.
3) The influence of shell and placement on the measured values of the parameters is comparatively studied in five working conditions.

The remainder of the paper is organized as follows. Section 2 introduces the related research in the past two decades. The hardware architecture and software design of the proposed IAQMS are presented in Section 3, respectively. Section 4 presents the monitoring results and analysis. Finally, Section 5 gives the critical conclusions and future outlook.

2. Literature reviews

There are a large number of literatures presented in the field of indoor air quality monitoring, which will be discussed in this section. A summary of related studies on the IAQMS in recent years is shown in Table 1. The table includes the four aspects: monitoring parameters, network, system architecture, and whether there is a shell.

In terms of monitoring parameters, the indoor air parameters monitored are different from study to study. Temperature and humidity are common parameters, that are related to people's thermal comfort in working and living places, and affect people's physiology and psychology [15]. Although not a pollutant per se, CO_2 is the second most popular parameter to measure indoors, especially in offices and classrooms [34]. Low concentrations of CO_2 in the air can inhibit the respiratory system, and cause fatigue and headache. However, higher levels can cause vomiting, dizziness, and nausea. Literature [22, 27, 35] paid attention to monitoring CO_2 concentrations in offices, laboratories, and living rooms. TVOC pollution levels in indoor environments were studied in [25, 26] based on WSN for factory and residential buildings, respectively. Because the higher TVOC concentration in buildings can irritate the skin, throat, nose, and eyes. In addition, O_3 is a colorless gas, an indispensable part of the atmosphere, and the main cause of various health diseases related to the respiratory system. Firdhous et al. [28] presented the O_3 concentrations monitoring system based on IoT in the office. Some literature [16, 21, 24, 29] focused on the study of CO and NO_2, which were related to the specific application locations. Special attention should be paid to the fact that particulate matter and formaldehyde are very harmful to humans, and have attracted the attention of researchers [15-17, 19, 23, 30].

In the choice of network, due to the flexibility of a wireless network, it is more and more used for data transmission in IAQMS. There are only two literature [16, 30] that adopt a wired method to collect IAQ sensor data. However, the data transmission performance of different types of wireless networks varies greatly, especially when transmitting in buildings. The transmission distance of Bluetooth adopted in [28] is 8-10m, which makes it only suitable for limited space [36]. In [21], a modular IoT platform for real-time IAQMS was presented based on Zigbee. The packet loss rate (PLR) was evaluated inside a library building at Qatar University. The results demonstrated that the PLR of Zigbee was more than 50% if there were double or triple concrete wall obstacles between the sending node and receiving node. The maximal distance was only 64 m. As one of the IoT communication technologies, LoRa presents a new communication technology that enables long-distance, long battery life, and large system capacity to meet the needs of the IoT [37]. In [38], the coverage and transmission performances of LoRa were explored in buildings in detail from round-trip time (RTT) delay and packet delivery rate (PDR) aspects in a 16-story building. The actual test results showed that LoRa can maintain more than 95% of the PDR despite the barrier of multiple wallboards on the same floor and the communication distance is less than 30 m. On the other hand, LoRa can transmit stably through 5 floors in the longitudinal direction. The excellent communication performance of LoRa makes it possible to obtain more and more applications in IAQMS, especially in large complex building systems. In addition to the above wireless networks suitable for data collection in the perceptual layer, WiFi, and 3G/4G networks were mainly used to achieve data transmission from IAQD to the local server or cloud platform [19, 23, 24].

The system architecture determines the flexibility and expansibility of the monitoring system. Traditionally, a datalogger is an early display device. Researchers usually need to take a datalogger to collect data on the spot [15-17]. Environmental data can be displayed on the datalogger in simple digital form or curve form. Then came the visual graphical interface of client/server (CS) architecture [25-30]. This kind of CS server can run on the computer, but it often needs to download software. It is difficult to realize the access of mobile terminals. Therefore, the local access is often used. With the advance of information technology, the IoT platform technology has developed rapidly in recent years. Monitoring systems based on IoT platform architecture are becoming more and more popular [19, 21-24]. The IoT platform can run on the terminal browser and be accessed by both computers and mobile phones, which makes the application of the monitoring system more flexible. Furthermore, the IoT platform can easily expand the application program interface to facilitate the later addition of algorithms, such as indoor air quality evaluation and prediction algorithms, to achieve comprehensive utilization of data.

In the study of equipment shell, most of the IAQDs developed in the literature [22, 23, 25-29, 35] do not add the shell or cover, while the equipment in the literature [15-17, 19, 21, 24, 30, 32] is covered by the shell. There is no research about the impact of the shell or cover on the measurement of

This work is licensed under a Creative Commons Attribution-NonCommercial-NoDerivatives 4.0 License. For more information, see https://creativecommons.org/licenses/by-nc-nd/4.0/

This article has been accepted for publication in IEEE Access. This is the author's version which has not been fully edited and
content may change prior to final publication. Citation information: DOI 10.1109/ACCESS.2023.3336706

IAQ. However, the microenvironment inside the shell changes after the power module and the sensor module work, although there are many vents on the surface of the shell, which has a certain impact on the IAQ measurement. To illustrate the influence of the presence or absence of the shell on the measurement of IAQ, we study the difference between the IAQD of the shell or not through the experimental method in the next section.

In the existing IoT-based system, it is usually discussed from the aspects of power consumption, RF design, and security. For example, Yang et al. proposed the use of unmanned aerial vehicles (UAV) as mobile PBs to provide energy signals to IoT nodes as needed [50]. These nodes use the collected energy to transmit their information to the reader through backscattering or active transmission. By jointly optimizing the transmission power and trajectory of the UAV, the backscattering reflection coefficient and active transmission power of the IoT node, and the time allocation of backscattering and active transmission, the total energy efficiency of the UAV driving the IoT node is maximized. Liu et al. applied non-orthogonal multiple access (NOMA) technology to achieve large-scale connectivity and studied how to use it to achieve energy-saving MEC in the Internet of Things network [51]. To maximize the energy efficiency of offloading while meeting the maximum tolerable delay, a joint radio and computational resource allocation problem considering intra-cell and inter-cell interference is proposed. Gupta et al. discussed the challenges associated with different RF designs, as well as their potential solutions and future research directions [52]. Zafari et al. discussed the positioning and localization of human users and their devices [53]. The advantages of the existing system proposed in the literature are emphasized. Compared with existing surveys, different systems were also evaluated in terms of energy efficiency, availability, cost, receiving range, latency, scalability, and tracking accuracy. Tewari et al. analyzed cross-layer heterogeneous integration issues and security issues, discussed the security issues of the Internet of Things as a whole, and tried to find solutions to these problems [54]. This paper compares the security issues of the Internet of Things and traditional networks and discusses the open security issues of the IoT.

The previous several researches have detailed various aspects. However, they still face some problems: 1) The measurement parameters are relatively simple, and only one indoor air quality parameter is concerned. This makes it necessary to install multiple sensors when measuring multiple parameters, which costs more time and money. 2) Data need to be collected and imported artificially, which wastes manpower and material resources and cannot measure these indoor air quality parameters in real time. 3) The previous research only verifies whether the data can be collected normally, and does not discuss the influence of different working conditions and the design of the instrument itself on the measurement parameters.

Table 1

A summary of related literature on IAQMS.

Ref.	Year	Monitoring parameters	Network	Architecture	Shell
25	2012	V	Zigbee	CS server	NA
27	2013	C_2	Zigbee	L-CS server	NA
26	2015	V	Zigbee	CS server	NA
35	2016	C_2	Radio module	L-display	No
28	2017	O_3	Bluetooth	CS server	No
23	2017	T, H, F	Zigbee, WiFi	IoT-plat	No
29	2017	T, H, C_1	Zigbee	L-CS server	No
22	2019	C_2	WiFi	IoT-plat	No
55	2022	T, H, P, V, F	WiFi	L-display	No
56	2021	C_1, C_2, P	WiFi	IoT-plat	No
57	2023	T, C_2, P	WiFi	IoT-plat	No
17	2013	C_2 , F	NA	datalogger	Yes
15	2016	T, H, C_2, P	3G	datalogger	Yes
21	2018	T, H,C_1,C_2,N	Zigbee	IoT-plat	Yes
32	2018	T, H, P,V,C_2	NA	L-display, SD store	Yes
19	2019	T,H,C_2,P,F	RS485, LoRa, WiFi, 4G, NB-IoT	IoT-plat	Yes
24	2019	C_1, C_4H_{10}	WiFi	IoT-plat	Yes
30	2020	P	Wired	L-CS server	Yes
16	2020	T,H,C_1,C_2,P	Wired	datalogger	Yes
58	2022	H, C_2,P	Wired	IoT-plat	Yes
59	2023	C_1, C_2, N,F	WiFi	IoT-plat	Yes
58	2023	C_2	WiFi	IoT-plat	Yes
Ours	2020	T, H,P,C_2,V,F	LoRa, 4G	IoT-plat	Yes

*T: temperature, H: humidity, C_1: CO, C_2: CO_2, V: TVOC, F: formaldehyde, N: NO_x, P: particulate matter; IoT-plat: IoT platform, L-CS: Local CS, L-display: Local display.

3. Indoor air quality monitoring system

The overall architecture of the indoor air quality monitoring system is described in Fig.1, which consists of a gateway and several sensor nodes. In the sensor layer, each deployed IAQD measurement site collects several IAQ parameters and sends them to the gateway through LoRa. The sensor gateway collects sensor data from IAQD through the Modbus protocol and posts them to the IoT web server in the format of MQTT. In the application layer, remote users can access real-time data in graphical or download historical data in tabular forms. The

This work is licensed under a Creative Commons Attribution-NonCommercial-NoDerivatives 4.0 License. For more information, see https://creativecommons.org/licenses/by-nc-nd/4.0/

This article has been accepted for publication in IEEE Access. This is the author's version which has not been fully edited and
content may change prior to final publication. Citation information: DOI 10.1109/ACCESS.2023.3336706

detailed hardware and software design of each part of the proposed IAQMS will be discussed in the following.

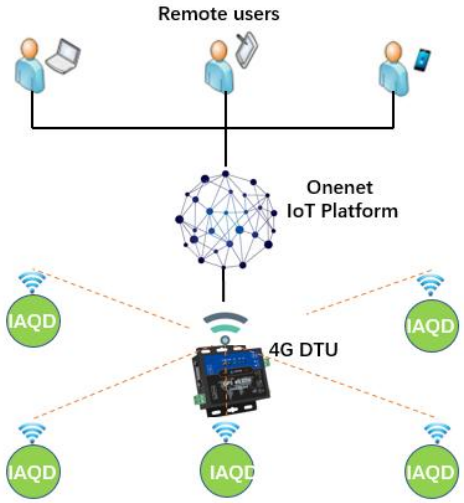

Fig.1. Architecture of indoor air quality monitoring system.

3.1 Hardware Design

3.1.1 IAQD design

Fig.2-(a) depicts a schematic diagram of the major components of an IAQD. For the measurement of primary pollutants, four pollutant sensors are selected, which can monitor five IAQ parameters. The ambient temperature and humidity sensors are chosen as thermal comfort parameters. The IAQD communicates wirelessly with the gateway through the LoRa wireless module. The STM32F103C8T6 (STM32) from STMicroelectronics Inc. is chosen as the microcontroller in this study, which incorporates 64 K of flash memory, 20 K of static RAM, and abundant peripheral interface resources, such as two 12-bit ADCs, a PWM timer, two I^2Cs and SPIs, three USARTs, a USB, and a CAN [39]. STM32 adopts a 48-pin package, which can be easily embedded into IAQD. The STM32 is programmed with Dynamic C software, an integrated development environment (IDE) that offers debugging support and a library of drivers. Fig.2-(b) shows the prototype of an IAQD, consisting of five on-board sensors (SHT31, PMS5003, WZ-S-K, S8 0053, and MiCS-VZ-89TE), onboard LoRa module (right side), and an RS485 interface, which is used to configure LoRa module.

SHT31 sensor is devoted to measuring the temperature and relative humidity. The module includes a resistive humidity sensing element and an NTC temperature measuring element. It communicates with the processor only through I2C and supports a 3 ~ 5 V power supply. PMS5003 sensor is used to monitor PM (PM2.5 and PM10). The working principle of the module is as follows: Firstly, the indoor air enters the module through the self-heating function, and the particulate matter is irradiated by the detection light emitted by the LED and then scattered. Then, the light pulse is converted into an electric pulse through the photoelectric converter to complete the identification of particulate matter. WZ-S-K is used to monitor HCHO. The module works according to the principle of electrochemistry. The current generated by the electrochemical oxidation process of the gas to be tested on the electrode is proportional to its concentration. The concentration of the gas to be tested can be determined by measuring the current. S8 0053 is used to monitor CO2. The module works according to the principle of non-dispersive infrared. The light passes through the measured gas in the optical path and passes through the narrow-band filter to reach the infrared detector. The concentration of the measured gas is determined by measuring the intensity of the infrared light entering the infrared sensor. MiCS-VZ-89TE sensor is utilized to measure TVOC. The module integrates advanced MOS principle sensors and intelligent detection algorithms to detect TVOC changes in narrow spaces, such as conference rooms and compartments.

The communication between STH31, MiCS-VZ-89TE, and STM32 is done through an I^2C bus, which only needs two wires to transmit information between devices connected to the bus. I^2C bus supports multi-node communication, and each device connected to the bus has a unique address. The data acquisition of S8 0053 is realized by STM32 via the PWM interface, with 0 to 100% duty cycle for 0 to 2000 ppm. Finally, the communication between WZ-S-K, PMS5003, and the microcontroller is achieved through two USARTs. In the communication process, the STM32 sends the acquisition instructions, and the returned messages from the WZ-S-K or PMS5003 contain the monitoring data.

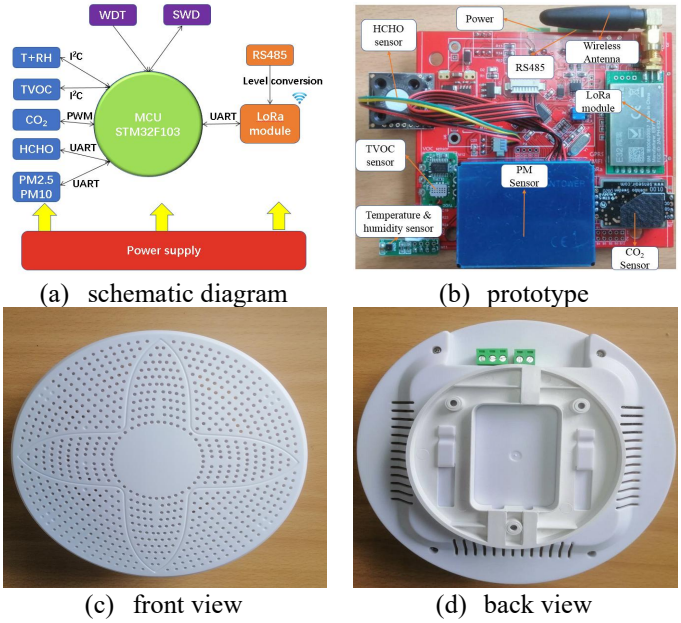

(a) schematic diagram (b) prototype

(c) front view (d) back view

Fig.2. IAQD sensor node.

The selection of a proper sensor is a relatively complicated issue, and there is always a trade-off among different factors. The application scenarios are diverse, such as lifetime, accuracy, power consumption, and availability [40]. In most cases, the parameters concerned by users are the accuracy of sensors. In this study, the selection standard of sensors is calibrated, as shown in Table 2.

This work is licensed under a Creative Commons Attribution-NonCommercial-NoDerivatives 4.0 License. For more information, see https://creativecommons.org/licenses/by-nc-nd/4.0/

This article has been accepted for publication in IEEE Access. This is the author's version which has not been fully edited and content may change prior to final publication. Citation information: DOI 10.1109/ACCESS.2023.3336706

Compared with the traditional wired method, the application of a wireless network makes IAQMS more convenient. Meantime, it reduces the construction, wiring, and other work requirements, and has strong flexibility. In this study, the LoRa is used as the communication module between IAQD and the gateway. In previous research, the LoRa module was tested with excellent penetration characteristics when deployed in the building [38]. E32-433T30D was chosen as the LoRa module, which is made by EBYTE Inc. in China, as shown in Fig.3-(a). More detailed information about E32-433T30D can be found in reference [38]. The communication level of the LoRa module is 3.3V, but the communication level of the RS485 configuration circuit is 5V. These two levels cannot communicate directly, so a level conversion circuit is designed, as illustrated in Fig.3-(b).

Table 2
Specifications of the sensors used in this study.

Para	Accur	N-range	Interface	Res-T (s)	Pc (mA)
T	±0.3℃	-40~125℃	I²C	T63 > 2	0.245
H	±2%	0-100%RH		T63 = 8	
P	± 10μg/m³	⩾1000μg/m³	UART	< 10	< 100
F	0.01ppm	0-2ppm	UART	T90 < 40	5
C_2	±40ppm	400-2000ppm	PWM	T90 = 120	18
V	1ppb	0-1000ppb	I²C	5	38

*Para: Parameter, Accur: Accuracy, N-range: Nominal Range, Res-T: Response Time, Pc: Power consumption; T90: rise time to 90% of final value, T63: rise time of 63% of the final valve

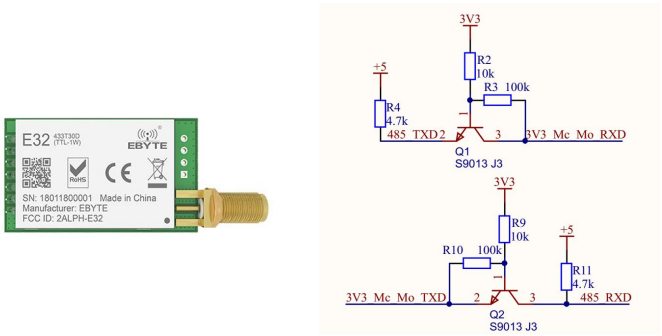

(a) LoRa module (b) level switching circuit

Fig.3. LoRa module and level switching circuit.

The prototype after assembly is shown in Fig.2-(c), with a diameter of 168 mm and a height of 5.1 mm. There is a separate back cover behind the prototype, which can be installed on the ceiling or hung on the wall. After adding the shell, the internal microenvironment of IAQD has changed, especially the internal temperature caused by heat dissipation is different from that of the outside, which will further affect the measurement data of the sensor. The presence of the shell will more or less affect the measurement, although there are some vents on it.

3.1.2 4G Modbus DTU

Fig.4. DTU module.

The main task of the IoT is the collection, transmission, and exchange of data between sensors at the perception layer and servers at the application layer. Data Transfer Unit (DTU) plays a vital role in the application of the IoT, acting as a communication bridge between the perception layer and the server. In this study, a 4G-DTU, TAS-LTE-395 is selected to realize two-way transparent transmission between IAQD and server in the cloud through Modbus protocol [41], as shown in Fig.4. In addition, TAS-LTE-395 also provides GPS/Beidou satellite positioning function to locate the location of IAQD. 4G DTU has its hardware watchdog circuit, which can be automatically reconnected after dropping the line. It can help users focus on the data acquisition of the sensing layer and software development of the application layer.

3.2 Software Design

This section describes the embedded software design of IAQD that is required to take a measurement and store it in the memory as Modbus RTU format. Each IAQD has its unique address on the Modbus Fieldbus. Fig.5 shows the workflow of software, which consists of the initialize module, collection module, package module, receiving and processing Modbus message module, sending module, configuration module, and WDG module.

This work is licensed under a Creative Commons Attribution-NonCommercial-NoDerivatives 4.0 License. For more information, see https://creativecommons.org/licenses/by-nc-nd/4.0/

This article has been accepted for publication in IEEE Access. This is the author's version which has not been fully edited and
content may change prior to final publication. Citation information: DOI 10.1109/ACCESS.2023.3336706

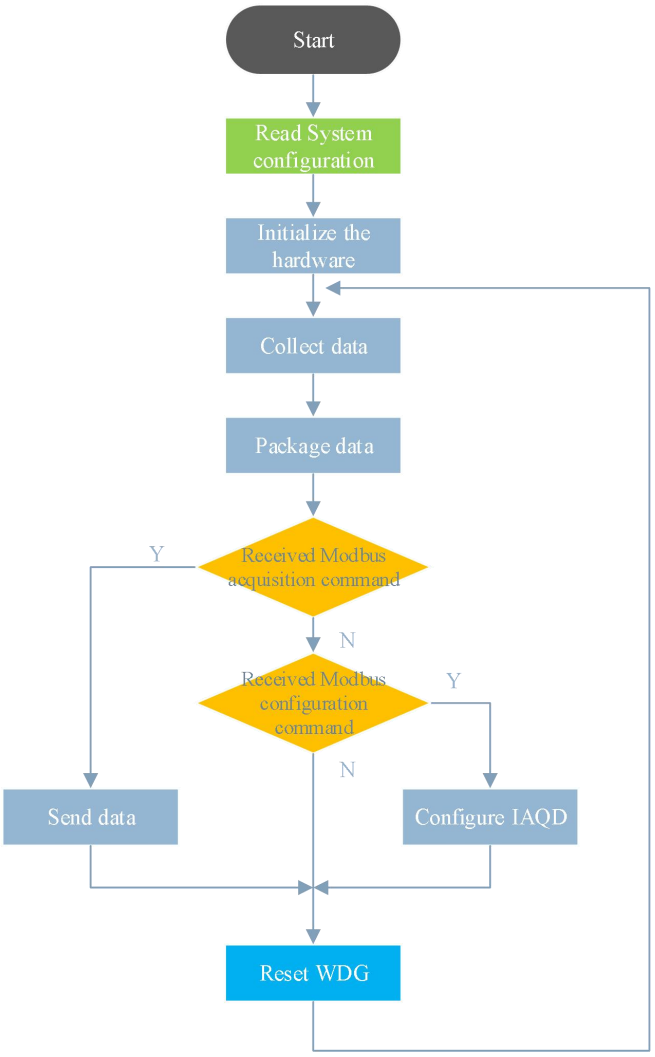

Fig.5. Workflow of the IAQD.

3.2.1 Initialization

This process includes the initialization of the system clock, UARTs, I²C interface, and flash memory. There are three UARTs of STM32. The first UART is used to communicate with the PM sensor. The second UART is used to communicate with the HCHO sensor. The third channel is used to communicate with DTU. The parameters of serial port configuration include baud rate, start bit, stop bit, and check bit. The corresponding configuration parameters in this study are 9600, N, 8, 1. The I²C interface is used to communicate with temperature/humidity and TVOC sensor, and the two sensors are distinguished by register addresses in SHT31 and MiCS-VZ-89TE. I²C bus supports multiple devices cascading, which reduces the hardware cost of the system and improves the work efficiency. To ensure the stability of I²C communication, a delay program should be added before operating another sensor after operating sensor.

3.2.2 Data acquisition and transmission

The microcontroller collects the temperature and humidity data from SHT31 through the I²C bus as 16-bit values (unsigned integer). These values are already linearized and compensated for temperature and supply voltage effects. Converting those raw values into a physical scale can be achieved using the following formulas [42].

Relative humidity conversion Formula (result in %RH):

$$RH=100\frac{S_{RH}}{2^{16}-1} \tag{1}$$

Temperature conversion Formula (result in °C):

$$T=175\frac{S_T}{2^{16}}-45 \tag{2}$$

Where, SRH and ST denote the raw sensor outputs of humidity and temperature, respectively.

With the same communication method, TVOC data can be obtained, as shown in Formula (3) [43].

$$TVOC=(S-13)\frac{1000}{229} \tag{3}$$

Where, S denotes the raw sensor output for TVOC.

S8 0053 provides two data interaction interfaces: serial communication and PWM. In this study, the PWM is chosen to read CO_2 data and reserve two UARTs for particulate matter and HCHO. The duty cycle of the PWM pin of the sensor 0-100% corresponds to 0-2000 ppm [44].

PMS5003 communicates with the microcontroller through the TTL serial port, the transport protocol of the host is shown in Table 3. By default, PMS5003 works in the active state and sends a data packet every second after powering on. PMS5003 has two working states, a low power consumption state and a working state. After entering the low power consumption state, it can save the energy consumption of the sensor and can be used in low-power monitoring occasions. After entering the working state, it can be divided into two modes: the active sending mode, which sends a data message every second. The other is the passive mode, which returns the data message after receiving the acquisition command sent by the microcontroller. In this study, the passive mode is selected, and PMS5003 is configured to work in the passive mode during initialization [45].

Table 3
Host protocol of PMS5003.

Start (2-bytes)	Command (1-byte)	Data1 (1-byte)	Data2 (1-byte)	Verify (2-bytes)
0x424D	CMD	DATH	DATAL	LRC

The reading process of the WZ-S-K module is similar to PMS5003, the transport protocol of WZ-S-K is shown in Table 4. The microcontroller sends fixed acquisition instructions, and receives the data returned by WZ-S-K through UART interrupt, and analyzes formaldehyde concentration [46].

Table 4
Protocol of WZ-S-K.

	0	1	2	3	4	5	6	7	8
S	0x FF	0x 01	0x 86	0x 00	0x 00	0x 00	0x 00	0x 00	0x 79

This work is licensed under a Creative Commons Attribution-NonCommercial-NoDerivatives 4.0 License. For more information, see https://creativecommons.org/licenses/by-nc-nd/4.0/

This article has been accepted for publication in IEEE Access. This is the author's version which has not been fully edited and
content may change prior to final publication. Citation information: DOI 10.1109/ACCESS.2023.3336706

R	0xFF	0x86	DH	DL	0x00	0x00	DH	DL	CLC

*S: Host send, R: WZ-S-K return, DH: concentration with the unit in μg/m^3, DL: concentration with the unit in ppb

STM32 periodically collects the data of the above mentioned five sensors and stores them according to the format of Modbus RTU protocol. The corresponding seven IAQ parameters are shown in Table 5. The application server in the OneNET sends data acquisition instructions through the 4G-DTU module as follows, and the data returned by IAQD are also interpreted in Table 5.

Master send: 01 03 00 00 00 07 04 08
IAQD return: 01 03 0E 01 30 02 C2 01 C4 00 3D 00 41 00 5C 00 6B C2 69

Table 5
IAQD modbus message analysis.

Para	T	H	CO_2	HCHO	TVOC	PM2.5	PM10
Register	0x00	0x01	0x02	0x03	0x04	0x06	0x07
Hex	0130	02C2	01C4	003D	0041	005C	006B
Dec	304	706	452	61	65	92	107
Value	30.4	70.6	452	0.061	0.065	92	107
Unit	℃	%	ppm	ppm	mg/m^3	μg/m^3	μg/m^3

3.2.3 Watchdog service

The watchdog service is a mechanism for detecting and recovering when STM32 failures. STM32 has a built-in watchdog module. When the watchdog service is enabled, a counter counts down from some initial value that can be configured. An interrupt signal will be generated. If the counter reaches zero, the microcontroller will reset. When developing the software, the watchdog module needs to be reinitialized at a suitable location to prevent the software from crashing.

3.3 OneNET Platform

OneNET is a public service-oriented and open cloud platform, independently researched and developed by CMIOT (China Mobile Internet of Things Co., Ltd.). It provides easy mass connection, cloud storage, information distribution, large data analysis, and other quality services for a variety of cross-platform IoT applications and industry solutions. Thereby, it can reduce the R&D, operation, and maintenance time for users, who can focus more on applications, and build a OneNET centered IoT ecological environment. OneNET platform provides relevant tools for device lifecycle management. It helps individuals and businesses quickly implement cloud management for large-scale devices. It opens third-party API interfaces and promotes the construction of personalized application system. It offers customized "and" APP and accelerates the generation of personalized intelligent applications.

OneNET is an efficient, stable, and secure open platform, that supports the equipment access of various industries and mainstream standard protocols, and provides IoT kits such as NB-IoT, MQTT, EDP, Modbus, HTTP, etc., to meet the requirements of various application scenarios. In this study, the Modbus protocol is chosen which is based on TCP connection, that is, Modbus TCP. OneNET encapsulates the data in TCP data for sending and receiving as a host. The simple transparent transmission capability achieved by DTU can realize the Modbus protocol communication between IAQD and the cloud platform. The structure diagram of Modbus protocol access to OneNET is shown in Fig.6.

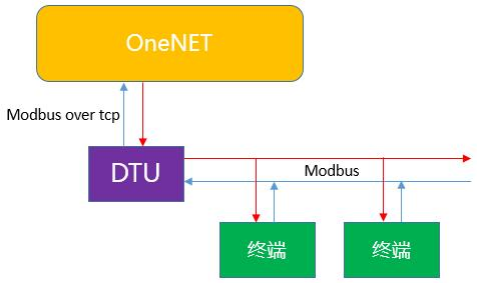

Fig.6. Structure diagram of Modbus protocol access to OneNET [47].

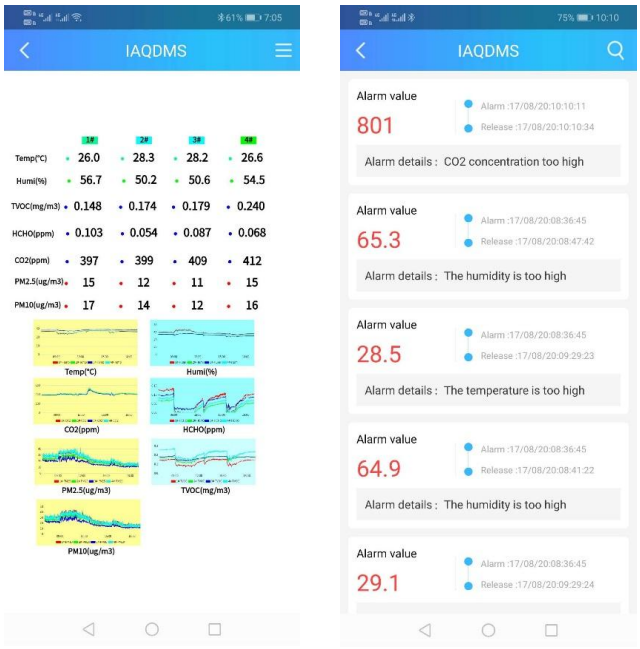

(a) real-time display (b) alarm notification

Fig.7. IAQMS application based on OneNET.

With the OneNET application editor, users can easily and quickly visualize device data streams by what you see is what you get (WYSIWYG) approach. The basic modules of the application editor include text display, line charts, histograms, maps, dashboards, etc. The application contains multiple pages, and the controls on each page are independent of each other, and support mobile page display. Fig.7 illustrates the GUI interfaces of the mobile terminal. On the dashboard, the air quality information can be shown in real-time in the form of text and charts.

3.4 Calibration

To ensure the accuracy of each measurement parameter, the

This work is licensed under a Creative Commons Attribution-NonCommercial-NoDerivatives 4.0 License. For more information, see https://creativecommons.org/licenses/by-nc-nd/4.0/

This article has been accepted for publication in IEEE Access. This is the author's version which has not been fully edited and
content may change prior to final publication. Citation information: DOI 10.1109/ACCESS.2023.3336706

IAQD is calibrated before the measurement. In the calibration process, the calibration instruments used are standard sensors, while ensuring that the standard sensor and the calibration sensor work in the same environment. The specific calibration process is as follows: 1) Check to confirm whether the standard sensor and calibration sensor can work properly. 2) Sensor connection. The standard sensor and the calibration sensor need to be connected to the same acquisition module and check whether the reading is normal. 3) Output detection. According to the calibration specification, the sensor output is read and recorded. 4) Calibration data processing. The calibration data is processed to obtain the sensor error. Through the above series of processes, all sensors in the IAQD are calibrated to ensure the accuracy of subsequent measurements.

To make the results more convincing, this study takes temperature and humidity as an example to show the calibration results, as shown in Fig.8. The results show that the error of the temperature sensor is 0.05 °C and the humidity sensor is 0.35 % after calibration, which fully meets the experimental requirements and can be used for subsequent different working conditions and shell experiments.

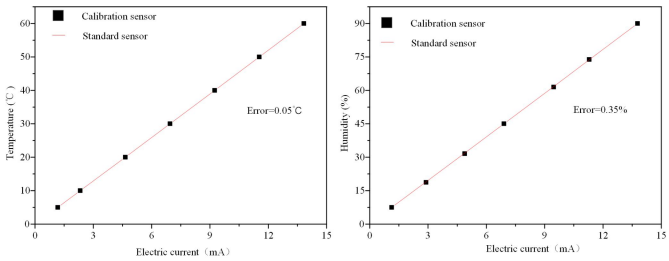

Fig.8. The calibration results of temperature and humidity sensors

4. Results and analysis

The measurement consistency and stability of the IAQD proposed in this study are verified through the experimental measurement methods in five different working conditions in the process of practical application, and the effect of adding a shell on the measurement of the sensor is comparatively studied. Due to different building types and uses, the IAQD is inevitably installed and works in different environments, so it is necessary to ensure that the IAQD can operate normally under these working conditions. However, due to the existence of sensors and power modules inside the housing, a lot of heat will be generated during the operation of the equipment, which may adversely affect the stable operation. Thus, the shell also needs to be discussed emphatically. In general, the discussion of the working conditions and shell in this study can ensure the reliability of the IAQD.

4.1 Experimental Setup

The experiments were conducted in an office on the 7th floor of the Innovation Building at Jinggangshan University to illustrate the overall functionality of the prototype system, and the shell impacts on the IAQ. The office (3 m × 6 m) has one researcher and there are chairs for two other visitors. During the experimental period, only one person was in the room. The main purpose of the experiment is to test the influence of adding a shell or not covering on the measurement value of IAQD. Four IAQDs (1# and 4# without cover, 2# and 3# with cover) are arranged, as shown in Fig.9. The four IAQDs are placed in the center of a table, which is two meters from the computer desk. In addition, the office is equipped with a central air conditioning system with air vents on the ceiling. The four IAQDs are not placed under the air vent.

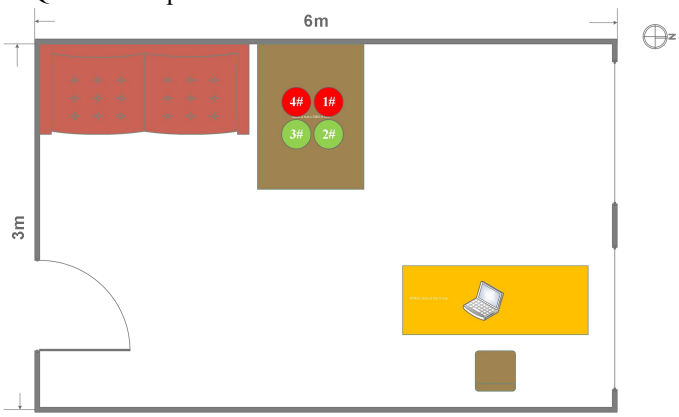

Fig.9. Four IAQDs are deployed in an office.

4.2 Results and Analysis

The experiments lasted for two days, between August 18 and August 19, 2020, with the data sampling every 30 seconds. All the IAQ data are downloaded from OneNET platform as the format of Excel. The whole experiment is divided into five working conditions (WCs), as represented in Fig.10-(a), and each WC lasts for 2 hours. During the non-experimental period, four IAQDs were collected and put together without cover. When the IAQDs were powered on to work, they needed 30 minutes to reach stable time due to the initial action needed for the sensors. Origin version 8.5 (OriginLab Corporation) was used to plot the results. Fig. 10-(b) to Fig. 10-(h) depict the changing trend of seven IAQ parameters on the whole.

When there is air circulation (WC-I, WC-II), the CO_2 concentration of IAQD-1# is higher than that of the other three conditions, although it is not the closest one to the people indoors. The concentration of IAQD-2# followed closely. The CO_2 concentration of IAQD-1# is kept the lowest in the other three conditions with no air circulation. The IAQD-2# with cover and closest to the researcher is always the highest. When there are people in the room, CO_2 is on the rise as a whole, and the rising speed in WC-I is the fastest. In addition, when the windows are opened, the fluctuation range of CO_2 is not volatile. It keeps horizontal fluctuation, and the concentration value is slightly higher than that under WCs without a man in the room.

The presence or absence of the shell has the most obvious impact on temperature and humidity. In the five WCs, obvious grouping phenomena can be seen. The changing trends of

This work is licensed under a Creative Commons Attribution-NonCommercial-NoDerivatives 4.0 License. For more information, see https://creativecommons.org/licenses/by-nc-nd/4.0/

This article has been accepted for publication in IEEE Access. This is the author's version which has not been fully edited and
content may change prior to final publication. Citation information: DOI 10.1109/ACCESS.2023.3336706

IAQD-1# and IAQD-4# are the same, and the changing trends of IAQD-2# and IAQD-3# are the same. Furthermore, temperature and humidity show obvious opposite trends. The test environment is located in a coastal city, and the summer air is humid. It can be seen that the humidity value of WC-II is close to 80%. The indoor temperature is generally higher than the comfortable temperature of 26 ℃, except for the working condition when the air conditioner is turned on.

The shell has no obvious grouping influence characteristics for the values monitored by the HCHO sensor. IAQD-1# has the highest HCHO value, which is much higher than the other three except for WC-II. When the doors and windows are opened and the air circulation is unobstructed, the HCHO values of the four IAQDs are all at low values. The fluctuation trends are consistent. In WC-III, when the door, window, and air condition system are closed, the values of the HCHO sensor with the housing of IAQD-2# and IAQD-3# have high consistency. Under WC-I, WC-IV, and WC-V, the data fluctuation range is relatively volatile.

The TVOC sensor is similar to the HCHO sensor, and the shell does not have obvious grouping influence characteristics. For IAQD-2# and IAQD-3#, the monitoring values of the two modules with shell are between the two modules without shell, IAQD-1 and IAQD-4#. On the whole, TOVC shows an upward trend except for WC-III.

The overall changing trend of PM2.5 and PM10 is highly consistent, and the value of PM10 is slightly higher than the value of PM2.5. Under WC-II, WC-III, and WC-V, it can be seen that the influence of the shell on the particulate matter is clearly distinguished. Especially for WC-II, when the door and window are opened and the air is circulating, the PM2.5 and PM10 pollutants enter the room from outside. At this time, the monitoring values of IAQD-2# and IAQD-3# with the shell are significantly lower than IAQD-1# and IAQD-4#.

The WC-I, WC-II, and WC-III were on August 18th, and the wind was gentle. However, the wind was a little bit stronger when WC-IV and WC-V on August 19th. So overall the data fluctuation of WC-IV and WC-V was greater than WC-I, WC-II, and WC-III. Next, the influence of whether the shell is added or not on the seven IAQ parameters under five WCs will be given in detail through quantitative analysis.

working condition	window	door	air conditioning	people
I	Close	Close	**Open**	1
II	**Open**	**Open**	Close	1
III	Close	Close	Close	0
IV	Close	**Open**	Close	1
V	**Open**	Close	Close	1

(a)

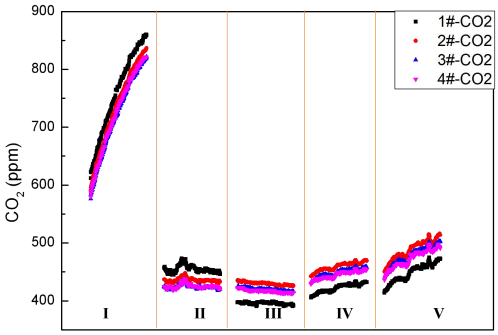

(b)

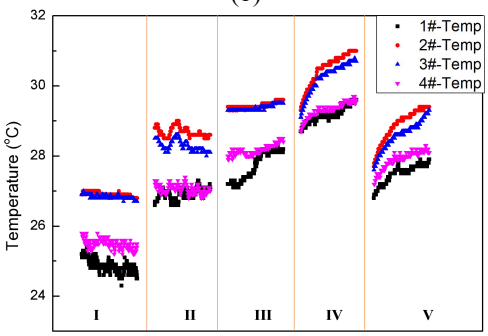

(c)

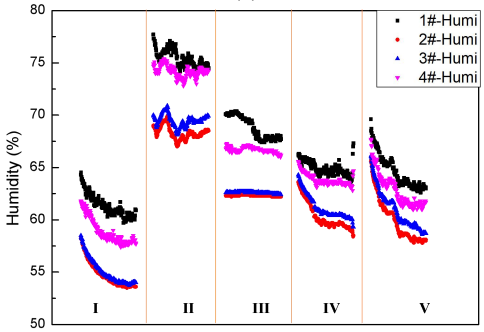

(d)

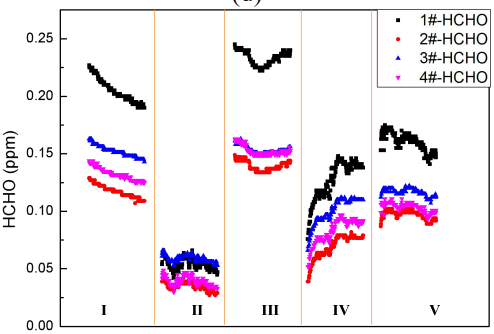

(e)

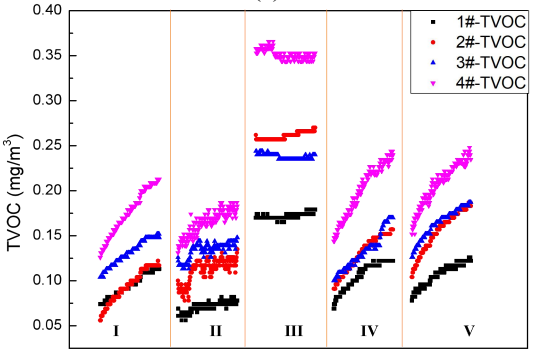

This work is licensed under a Creative Commons Attribution-NonCommercial-NoDerivatives 4.0 License. For more information, see https://creativecommons.org/licenses/by-nc-nd/4.0/

This article has been accepted for publication in IEEE Access. This is the author's version which has not been fully edited and
content may change prior to final publication. Citation information: DOI 10.1109/ACCESS.2023.3336706

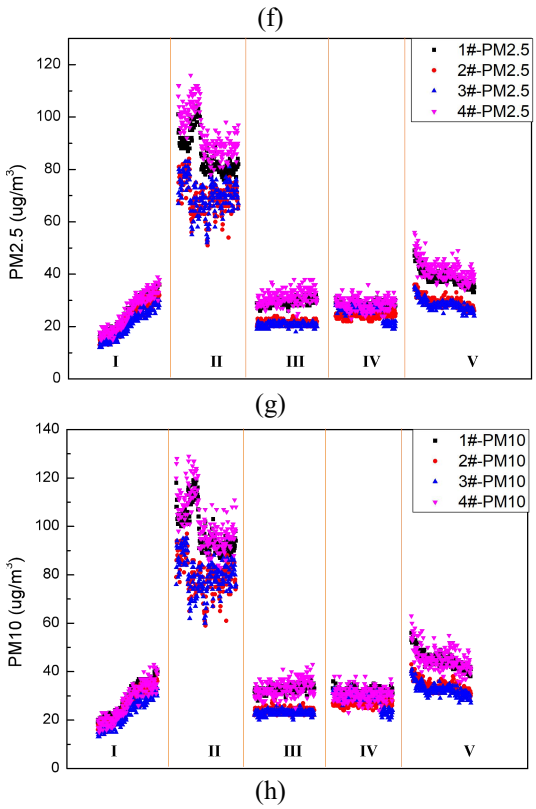

Fig.10. The changing trend of seven IAQ parameters.

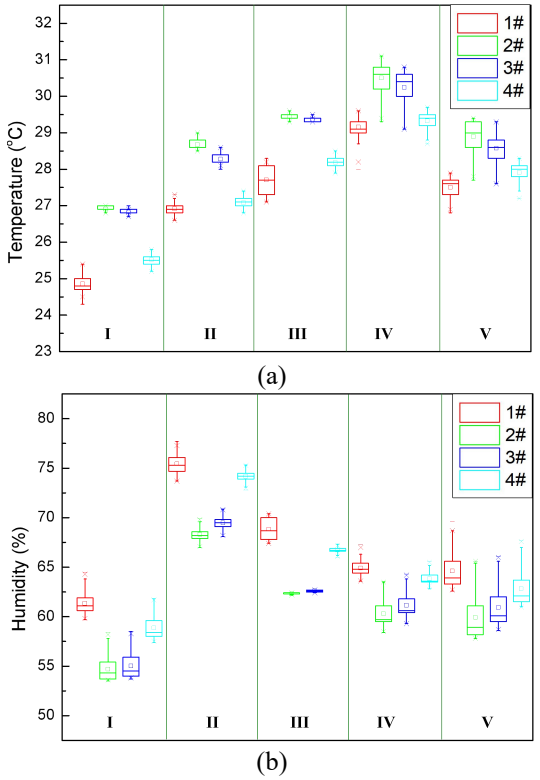

Fig.11. Temperature (a) and humidity (b) of the four IAQDs in five WCs. The box plots show the 25,50 and 75 percentiles, with the minimum, average (square), and maximum values.

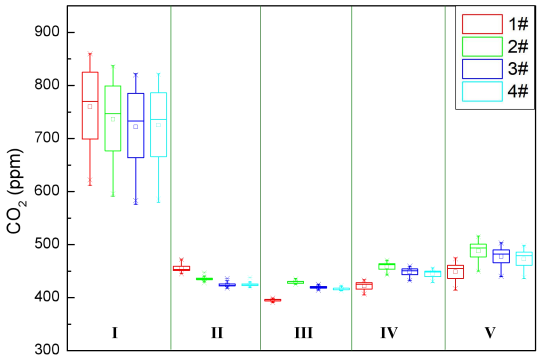

Fig.12. CO_2 of the four IAQDs in five WCs. The box plots show the 25,50 and 75 percentiles, with the minimum, average (square), and maximum values.

4.2.1 Temperature

Fig.11-(a) presents the temperature values of the four IAQDs in five WCs, with a mean value of 29.9±1.8 ℃, ranging from 24.9±0.5 ℃ (IAQD-1# in WC-I) to 30.1±1.1 ℃ (IAQD-2# in WC-IV). The average temperature values of IAQD-2# and IAQD-3# with shell are 2.7 ℃ higher than IAQD-1# and IAQD-4# without shell. In addition, the temperature of IAQD-1# is a little lower than IAQD-4# due to the location of IAQD-1# being closer to the windows and air conditioning vents. Considering indoor air quality standard (GB/T18883 − 2022) that establishes a temperature range for the occupants' comfort in summer between 22 and 28 ℃ [48]. Only WC-I can ensure that the indoor temperature is lower than 28 ℃ when the air condition system is turned on.

4.2.2 Humidity

Fig.11-(b) depicts the humidity values of the four IAQDs in five WCs, with a mean value of 59.0±1.1%, ranging from 56.0±3.4% (IAQD-2# in WC-I) to 76.1±2.3% (IAQD-1# in WC-II). The average humidity values of IAQD-1# and IAQD-4# without shell are 4.7% higher than IAQD-2# and IAQD-3# with shell. In addition, the IAQD-1# always has the highest humidity value. Similarly, the national standard (GB/T18883 − 2022) indicates that the suitable indoor humidity range is 40-80 %. It can be seen from the results that the humidity measurement values under different working conditions meet the requirements.

4.2.3 CO_2

Compared with the placement of IAQD, the shell has little effect on CO_2, which is different from temperature and humidity, as shown in Fig.12. When someone is indoors (WC-I, II, IV, V), CO_2 shows an upward trend overall. Due to the gentle wind on the 18th, the CO_2 concentration values of IAQD-1# and IAQD-2# closest to the desk are relatively higher than IAQD-3# and IAQD-4# in WC- I and II, with the average value of 3.5% higher. The wind was slightly stronger on the 19th, so the IAQD-1# near the window has the lowest CO_2 value, which is 5% lower than the other three IAQDs. When there is no one in the room (WC-III), the CO_2 values of the four IAQDs fluctuate slightly, and the difference between the maximum and

This work is licensed under a Creative Commons Attribution-NonCommercial-NoDerivatives 4.0 License. For more information, see https://creativecommons.org/licenses/by-nc-nd/4.0/

This article has been accepted for publication in IEEE Access. This is the author's version which has not been fully edited and
content may change prior to final publication. Citation information: DOI 10.1109/ACCESS.2023.3336706

minimum values of CO_2 is only 10 ppm. The upper limit of CO_2 in national standards is 1000 ppm. According to the measurement results under different working conditions, it can be seen that the measurement value of WC-I is far from other working conditions because there is no air circulation, but it still meets the indoor air quality requirements.

4.2.4 HCHO

Overall, the mean HCHO level is 0.164±0.088 mg/m^3, ranging from 0.034±0.007 mg/m^3 (IAQD-2# in WC-II) to 0.243±0.004 mg/m^3 (IAQD-1# in WC-III). High temperature in summer is the main cause of HCHO emission, especially when the temperature reaches 30 ℃. The high levels of HCHO indoors may originate from emissions of household materials and consumer products [49]. The upper limit of HCHO in the indoor air quality standard (GB/T18883 − 2002) is 0.1 mg/m^3. It can be seen from Fig.13-(a) that only WC-II can meet the standard, with an average value of 0.047 mg/m^3. The average values of other conditions are 0.152 mg/m^3 for WC-I, 0.171 mg/m^3 for WC-III, 0.105 mg/m^3 for WC-IV, 0.12 mg/m^3 for WC-V. Although turning on the air condition can lower the temperature and ensure thermal comfort, the enclosed space cannot emit HCHO, which is still harmful to the human body. In addition, the measured value of formaldehyde of each IAQD is related to its microenvironment, and the shell has little effect on it. The upper limit of HCHO in national standards is 0.08 mg/m^3, and only WC-II meets the requirements. This also shows that windows should be opened for air circulation as long as possible instead of turning on the air conditioning system to ensure the indoor air quality.

*4.2.5*TVOC

It can be seen that the TVOC values of IAQD-2# and IAQD-3# with shell are similar, while the values of IAQD-1# and IAQD-4# without shell are quite different from Fig.13-(b). Especially in WC- III, the average value of TVOC of IAQD-2# differs from IAQD-3# by only 0.023 mg/m^3, while the average value of IAQD-1# and IAQD-4# differs by 0.181 mg/m^3. The average TVOC under five WCs is 0.16 mg/m^3, which is lower than the national standard of 0.6 mg/m^3 [48].

4.2.6 Particulate matter (PM)

Fig.14 presents the statistics value of particulate matter. It can be seen that the highest concentrations of PM2.5 and PM10 have exceeded 100 μg/m^3 in WC-II when the window and the door are opened. In the other four WCs, the particulate matter concentration changes little, the average values of PM2.5 and PM10 are 27.7 μg/m^3 and 30.8 μg/m^3, respectively. However, all these measurement values are greater than the national standards (PM2.5 is less than 0.05μg/m^3, PM10 is less than 0.1μg/m^3). This also shows that indoor air circulation is needed. Considering that direct air circulation in WC-II will increase the concentration of particulate matter. Therefore, it is necessary to filter the air before entering the house. In WC-II, the average values of IAQD-2# and IAQD-3# with shell are 29.4% lower than that of IAQD-1# and IAQD-4# without shell. Under these circumstances, the shell is equivalent to a protective cover for the PM sensor. It can effectively isolate the intrusion of external particles, but the accuracy of the measurement data is reduced. Furthermore, it is not a wise choice to open the window when the outdoor particle concentration is higher [19]. Compared with WC-II, the particulate matter concentration fluctuation of other WCs is not obvious, but the average values of IAQD-2# and IAQD-3# are still lower than that of IAQD-1# and IAQD-4#, which also indicates that the addition of the shell has an influence on the measurement results of particulate matter. In addition, the overall concentration of PM10 is 11.9% higher than that of PM2.5.

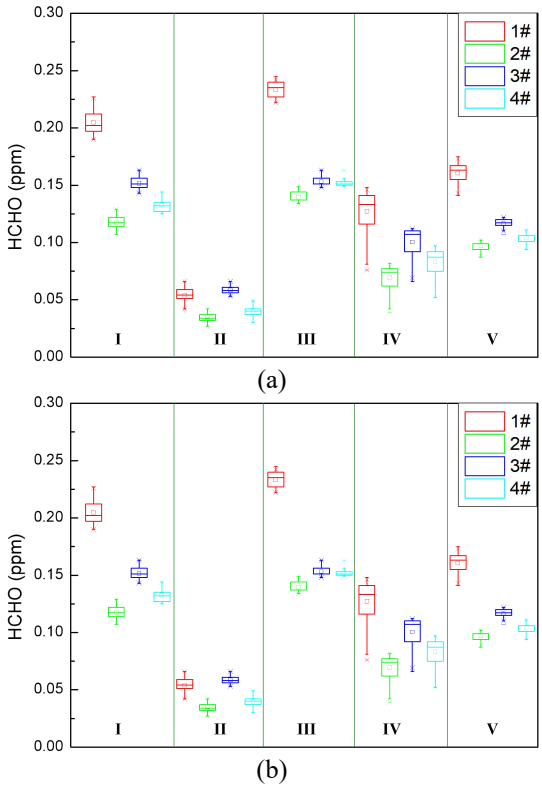

(a)

(b)

Fig.13. HCHO (a) and TVOC (b) of the four IAQDs in five WCs. The box plots show the 25,50 and 75 percentiles, with the minimum, average (square), and maximum values.

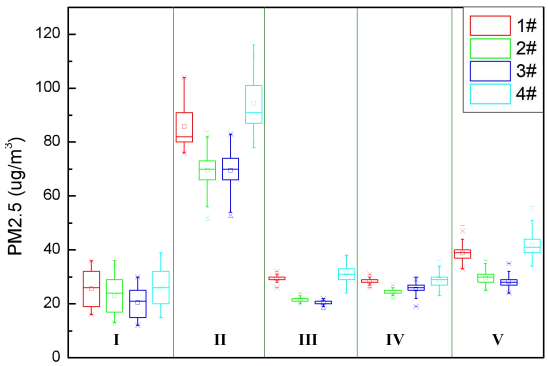

(a)

This work is licensed under a Creative Commons Attribution-NonCommercial-NoDerivatives 4.0 License. For more information, see https://creativecommons.org/licenses/by-nc-nd/4.0/

This article has been accepted for publication in IEEE Access. This is the author's version which has not been fully edited and
content may change prior to final publication. Citation information: DOI 10.1109/ACCESS.2023.3336706

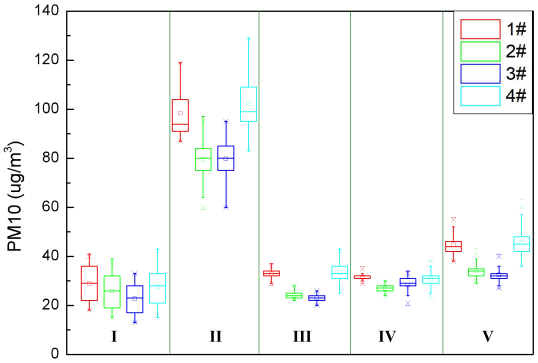

(b)

Fig.14. PM2.5 (a) and PM10 (b) of the four IAQDs in five WCs. The box plots show the 25,50 and 75 percentiles, with the minimum, average (square), and maximum values.

4.3 Discussions

In this study, IoT devices are composed of multiple components such as a gateway and several sensor nodes. Although the energy consumption of a single component is low, the IoT system requires a large number of components, which means that the energy consumption is very high. Therefore, energy consumption management is particularly important in IoT devices. Meantime, energy consumption management can also improve the overall performance and sustainability of IoT devices. To reasonably manage and optimize the energy consumption in the IoT, some appropriate methods are adopted: 1) Low power processor. The operating power consumption of low power processors is very low, which can ensure that the energy consumption of the entire IoT device is at a low level. 2) Energy saving sensor. Compared with traditional sensors, energy-saving sensors have very low energy consumption in the dormant state. This can avoid the waste of energy consumption when the sensor is running. The energy-saving sensor also has another advantage, that is, its sleep time can be adjusted by parameters to better adapt to the practical use environment in the design stage. 3) Energy consumption optimization algorithm. The energy consumption optimization algorithm can consider the network topology, data exchange flow, and equipment running time of the whole system to realize the optimal management of energy consumption.

The energy consumption optimization algorithm is the most effective way to reduce energy consumption when the IoT devices have been designed. Common energy consumption optimization algorithms include load balancing, data pruning, etc. In the application process of the data pruning algorithm, the time for the sensor to transmit data can be appropriately extended when the indoor or outdoor changes are not dramatic so that the sensor can remain dormant and reduce the energy consumption of the IoT device.

With an increasingly severe global energy shortage, renewable energy has attracted considerable attention. Solar energy, as one of the most important renewable energy sources, has been well-developed in recent years. To realize the efficient use of solar energy, solar energy storage technology has been developed. In the existing photovoltaic equipment, the electricity generated by solar energy can be stored. Then the IoT device wires are connected to the energy storage device and the municipal power grid at the same time. During the normal operation of the IoT device, the power of the energy storage device maintains its operation. When there is not enough power in the energy storage device, it is switched to the municipal power grid. The energy storage device is monitored in real time and then switched back after some power is stored in the energy storage device. This makes the energy consumed by IoT devices come from solar energy, reducing municipal electricity consumption.

5. Conclusions

In this paper, we designed and implemented a real-time indoor air quality monitoring system based on LoRa WSN, DTU, and OneNET, which is comprised of an embedded microcontroller, and five indoor sensors to monitor seven IAQ parameters. The system was deployed and tested in an office of Jinggangshan University, and the influence of different placement positions and the shell on monitoring data was compared and analyzed.

In different working conditions, the IAQD can measure the data stably. Although the measured data fluctuates to some extent due to the influence of doors and windows, air conditioning, and personnel, the changing trend of the data is still measured accurately. For a fixed sensor, the temperature is the lowest and the humidity is the highest when the air conditioner is turned on (WC-1). However, the CO2 concentration rises slowly due to the breathing of indoor personnel when the doors and windows are closed and there are personnel. For HCHO and TVOC, they will gradually increase with the increase of temperature in different working conditions, and the concentration is the lowest when the doors and windows are completely opened (WC-2). Meantime, the PM2.5 and PM10 come from outdoor pollution gas, and their concentration is the highest in the working condition 2. In summary, no matter how the working conditions change, the IAQD can record the change process, which shows the reliability of transmission based on the Internet of Things.

The shell has the greatest influence on temperature and humidity among the seven parameters monitored by this study. When the system is turned on, the sensors and power modules inside the housing begin to radiate heat, causing the temperature of the microenvironment inside the housing to increase and the humidity to decrease. Furthermore, the shell has little effect on the data of CO_2, HCHO, and TVOC. These three parameters are related to the environment wind speed and the placement of the sensor, and the measured data is inversely proportional to the wind speed. Finally, the shell also has a certain influence on the measurement results of particulate matter. When indoor and outdoor air circulates, the monitoring data of PM2.5 and PM10 with the shell are 29.4% lower than the data without the shell.

The presented IAQD is easy to deploy in buildings, and the LoRa WSN makes it possible for large-scale applications in one

This work is licensed under a Creative Commons Attribution-NonCommercial-NoDerivatives 4.0 License. For more information, see https://creativecommons.org/licenses/by-nc-nd/4.0/

This article has been accepted for publication in IEEE Access. This is the author's version which has not been fully edited and
content may change prior to final publication. Citation information: DOI 10.1109/ACCESS.2023.3336706

or more buildings. In addition, the browser/server structure of the application software is flexible and can be accessed by users anywhere with a network. The designed platform can be easily modified to integrate more indoor environment parameters, such as illumination, noise, etc. By using this presented IAQMS, we can detect unhealthy situations in real-time and send a reminder message to the user.

In the future, we will focus on the verification of monitoring data of different sensors under different working conditions by using a machine learning algorithm and predict the IAQ of the monitoring system. In addition, we will propose a comprehensive evaluation method of IAQ based on fuzzy comprehensive evaluation, and carry out practical application and verification research on office environment, student dormitory, residential environment, and other occasions.

Acknowledgements

This research is supported by The Culture, Art and Science Planning Project of Jiangxi Province (No. YG2022096).

References

[1] WHO, 2018b. How air pollution is destroying our health [Online]. Available: https://www.who.int/air-pollution/news-and-events/how-air-pollution-is-destroying-our-health

[2] Ostro B, Spadaro J V, Gumy S, et al. "Assessing the recent estimates of the global burden of disease for ambient air pollution: methodological changes and implications for low- and middle-income countries," *Environ. Res.*, vol. 166, pp. 713-725, Oct. 2018.

[3] WHO, 2018a. Ambient (outdoor) air pollution [Online]. Available: https://www.who.int/news-room/fact-sheets/detail/ambient-(outdoor)-air-quality-and-health

[4] Klepeis N E, Nelson W C, Ott W R, et al. "The National Human Activity Pattern Survey (NHAPS): A resource for assessing exposure to environmental pollutants," *J. Expo. Sci. Environ. Epidemiol.*, vol. 11, no. 3, pp. 231-252, Mar. 2001.

[5] Lee S, Lam S, Fai H K. "Characterization of VOCs, ozone, and PM 10 emissions from office equipment in an environmental chamber," *Build. Environ.*, vol. 36, no. 7, pp. 837–842. Aug. 2001.

[6] Seguel J M, Merrill R, Seguel D, et al. "Indoor air quality," *Am. J. Lifestyle Med.*, vol. 11, no. 4, pp. 284–2895, Jun. 2016.

[7] Yang L., Li W., Ghandehari M., et al. "People-centric cognitive internet of things for the quantitative analysis of environmental exposure," *IEEE Internet Things J.*, vol. 5, no. 4, pp. 2353-2366, Sept. 2017.

[8] Lei L, Chen W, Xue Y, et al. "A comprehensive evaluation method for indoor air quality of buildings based on rough sets and a wavelet neural network," *Build. Environ*., vol. 162, Sept. 2019.

[9] Saini J, Dutta M, Marques G. "A comprehensive review on indoor air quality monitoring systems for enhanced public health," *Sustain. Environ. Res.*, vol. 30, no. 6, Jan. 2020.

[10] Baek S, Kim Y, Perry R. "Indoor air quality in homes, offices and restaurants in Korean urban areas-indoor/outdoor relationships," *Atmos. Environ.*, vol. 31, no. 4, pp. 529–544, Feb. 1997.

[11] Yu B, Hu Z B, Liu M, et al. "Review of research on air-conditioning systems and indoor air quality control for human health," *Int. J. Refrig.*, vol. 32, no. 1, pp. 3–20, Jan. 2009.

[12] Lee S C, Li W, Chan L Y. "Indoor air quality at restaurants with different styles of cooking in metropolitan Hong Kong," *Sci. Total Environ.*, vol. 279, no. 1-3, pp. 181-193, Nov. 2001.

[13] Li W, Lee S C, Chan L Y. "Indoor air quality at nine shopping malls in Hong Kong," *Sci. Total Environ.*, vol. 273, no. 1–3, pp. 27-40, Jun. 2001.

[14] Guo H, Lee S C, Chan L Y. "Indoor air quality investigation at air-conditioned and non-air-conditioned markets in Hong Kong," *Sci. Total Environ.*, vol. 323, no. 1–3, pp. 87-98, May 2004.

[15] Carre A, Williamson T. "Design and validation of a low cost indoor environment quality data logger," *Energy Build.*, vol. 158, pp. 1751-1761, Jan. 2018.

[16] Sumei L, Qing C, X.W. Z, et al. "Improving indoor air quality and thermal comfort in residential kitchens with a new ventilation system," *Build. Environ.*, vol. 180, Aug. 2020.

[17] Plaisance H, Blondel A, Desauziers V, et al. "Field investigation on the removal of formaldehyde in indoor air," *Build. Environ.*, vol. 70, pp. 277-283, Dec. 2013.

[18] Langer S, Beko G, Bloom E, et al. "Indoor air quality in passive and conventional new houses in Sweden," *Build. Environ.*, vol. 93, pp. 92-100, Nov. 2015.

[19] L. Zhao, W. Wu, S. Li. "Design and Implementation of an IoT-Based Indoor Air Quality Detector With Multiple Communication Interfaces," *IEEE Internet Things J.*, vol. 6, no. 6, pp. 9621-9632, Dec. 2019.

[20] L. Zhao, G. Wang, L. Ma, et al. "A Modular Indoor Air Quality Monitoring System Based on Internet of Thing," *in Proc CSPS*, Urumqi, China, Jul. 2019, pp. 1766–1772.

[21] Benammar M, Abdaoui A, Ahmad S H, et al. "A Modular IoT Platform for Real-Time Indoor Air Quality Monitoring," *Sensors*, vol. 18, no. 2, Feb. 2018.

[22] Marques G, Ferreira C R, Pitarma R. "Indoor Air Quality Assessment Using a CO2 Monitoring System Based on Internet of Things," *J. Med. Syst.*, vol. 43, no. 3, Feb. 2019.

[23] He J, Xu L, Wang P, et al. "A high precise E-nose for daily indoor air quality monitoring in living environment," *Integration-VLSI J.*, vol. 58, pp. 286–294, Jun. 2017.

[24] Marques G, Pitarma R. "A Cost-Effective Air Quality Supervision Solution for Enhanced Living Environments through the Internet of Things," *Electronics*, vol. 8, no. 2, Feb. 2019.

[25] Manes G, Collodi G, Fusco R, et al. "A wireless sensor network for precise volatile organic compound monitoring," *Int. J. Distrib. Sens. Netw.*, vol. 8, no. 4, Feb. 2012.

[26] Peng C, Qian K, Wang C. "Design and Application of a VOC-Monitoring System Based on a ZigBee Wireless Sensor Network," *IEEE Sens. J.*, vol. 15, no. 4, pp. 2255-2268, Apr. 2015.

This work is licensed under a Creative Commons Attribution-NonCommercial-NoDerivatives 4.0 License. For more information, see https://creativecommons.org/licenses/by-nc-nd/4.0/

This article has been accepted for publication in IEEE Access. This is the author's version which has not been fully edited and
content may change prior to final publication. Citation information: DOI 10.1109/ACCESS.2023.3336706

[27] Preethichandra D M. "Design of a smart indoor air quality monitoring wireless sensor network for assisted living," *in Proc I2MTC*, Minneapolis, MN, USA, May 2013, pp. 1306–1310.
[28] Firdhous M F M, Sudantha B H, Karunaratne P M. "IoT enabled proactive indoor air quality monitoring system for sustainable health management," *in Proc ICCCT*, Chennai, India, Feb. 2017, pp.216-221.
[29] Alhmiedat T, Samara G. "A Low Cost ZigBee Sensor Network Architecture for Indoor Air Quality Monitoring," *Int. J. Comput. Sci. Inf. Secur.*, vol. 15, no. 1, pp. 140-144, Jan. 2017.
[30] Wang Z, Delp W W, Singer B C. "Performance of low-cost indoor air quality monitors for PM2.5 and PM10 from residential sources," *Build. Environ.*, vol. 171, Mar. 2020.
[31] Abraham S, Li X. "A cost-effective wireless sensor network system for indoor air quality monitoring applications," *Procedia Comput. Sci.*, vol. 34, pp. 165–171, Aug. 2014.
[32] Tiele A, Esfahani S, Covington J A. "Design and development of a low-cost, portable monitoring device for indoor environment quality," *J. Sens.*, vol. 2018, no. 2018, pp. 1–14, Mar. 2018.
[33] Chojer H , Branco P T B S , Alvim-Ferraz M C M , et al. "Development of low-cost indoor air quality monitoring devices:Recent advancements," *Sci. Total Environ.*, vol. 727, Jul. 2020.
[34] Branco P T B S, Nunes R A O, Alvim-Ferraz M C M, et al. "Children's exposure to indoor air in urban nurseries – part II: gaseous pollutants' assessment," *Environ. Res.*, vol. 142, pp. 662–670, Oct. 2015.
[35] Spachos P, Hatzinakos D. "Real-time indoor carbon dioxide monitoring through cognitive wireless sensor networks," *IEEE Sensors J.*, vol. 16, no. 2, pp. 506-514, Jan. 2016.
[36] Ray P P. "A Survey on Internet of Things Architectures," *J. King Saud Univ.-Comput. Inf. Sci.*, vol. 30, no. 3, pp. 291–319, Jul. 2018.
[37] Zhang X, Zhang M, Meng F, et al. "A Low-Power Wide-Area Network Information Monitoring System by Combining NB-IoT and LoRa," *IEEE Internet Things J.*, vol. 6, no. 1, pp. 590–598, Feb. 2019.
[38] R. Liang, L. Zhao, P. Wang. "Performance Evaluations of LoRa Wireless Communication in Building Environments," *Sensors*, vol. 20, no. 14, Jul. 2020.
[39] [Online]. Available: https://pdf1.alldatasheet.com/datasheet-pdf/view/201596/stmicroelectronics/stm32f103c8t6.html
[40] Kim J, Chu C, Shin S. "ISSAQ: An Integrated Sensing Systems for Real-Time Indoor Air Quality Monitoring," IEEE Sens. J., vol. 14, no. 12, pp. 4230-4244, Dec. 2014.
[41] [Online]. Available: https://www.tastek.cn/Product/47
[42][Online]. Available: https://www.sensirion.com/fileadmin/user_upload/customers/sensirion/Dokumente/2_Humidity_Sensors/Datasheets/Sensirion_Humidity_Sensors_SHT3x_Datasheet_digital.pdf
[43] [Online]. Available: https://www.sgxsensortech.com/content/uploads/2016/07/MiCS-VZ-89TE-V1.0.pdf
[44] [Online]. Available: https://www.driesen-kern.de/downloads/modul_senseair_s8_004_8_0053_4sec_s80021.pdf
[45] [Online]. Available: https://www.thaieasyelec.com/downloads/ESEN298/PMS5003ST_Datasheet.pdf
[46] [Online]. Available: http://szprosense.com/en/product_show.php?id=91
[47] [Online]. Available: https://open.iot.10086.cn/en/doc/art370.html
[48] [Online]. Available: https://webstore.ansi.org/Standards/SPC/GB188832002#PDF
[49] Canha N, Lage J, Candeias S, et al. "Indoor air quality during sleep under different ventilation patterns," *Atmos. Pollut. Res.*, vol. 8, no. 6, pp. 1132-1142, Nov. 2017.
[50] Yang H, Ye Y, Chu X, et al. "Energy Efficiency Maximization for UAV-Enabled Hybrid Backscatter-Harvest-Then-Transmit Communications," *IEEE transactions on wireless communications*, 21(5), pp. 2876–2891, 2022.
[51] Liu B, Liu C and Peng M. "Resource Allocation for Energy-Efficient MEC in NOMA-Enabled Massive IoT Networks," *IEEE journal on selected areas in communications*, 39(4), pp. 1015–1027, 2021.
[52] Gupta B.B. and Quamara M. "An overview of Internet of Things (IoT): Architectural aspects, challenges, and protocols," *Concurrency and computation*, 32(21), p. n/a, 2020.
[53] Zafari F, Gkelias A and Leung K.K. "A Survey of Indoor Localization Systems and Technologies," *IEEE Communications surveys and tutorials*, 21(3), pp. 2568–2599, 2019.
[54] Tewari A. and Gupta B.B. "Security, privacy and trust of different layers in Internet-of-Things (IoTs) framework," *Future generation computer systems*, vol. 108, pp. 909–920, 2020
[55] Wang, C., Liu, H., Ji, J., and Wu, Y. A Design of Indoor Air-Quality Monitoring System. Journal of Physics. Conference Series, 2366(1), 12011,2022.
[56] Sung, W. T., and Hsiao, S. J. Building an indoor air quality monitoring system based on the architecture of the Internet of Things. EURASIP Journal on Wireless Communications and Networking, 2021, 1-41.
[57] Gandara, M., Saputro, N., & Naa, C. Design of an internet of things-based low-cost EIAQI-based indoor air quality monitoring system. AIP Conference Proceedings, 2706(1), AIP Conference Proceedings, 2023, Vol.2706 (1).
[58] Ramachandraarjunan, S., Perumalsamy, V., and Narayanan, B. IoT based artificial intelligence indoor air quality monitoring system using enabled RNN algorithm techniques. Journal of Intelligent & Fuzzy Systems, 43(3), 2853-2868, 2022.
[59] Guerrero-Ulloa, G., Andrango-Catota, A., Abad-Alay, M., Hornos, M., and Rodríguez-Domínguez, C. Development and Assessment of an Indoor Air Quality Control IoT-Based System. Electronics (Basel), 12(3), 608, 2023.
[60] Zhu, Y., Al-Ahmed, S., Shakir, M., and Olszewska, J. LSTM-Based IoT-Enabled CO2 Steady-State Forecasting for Indoor Air Quality Monitoring. Electronics (Basel), 12(1), 107, 2023.

LIDONG PANG received the M.S. degree in heating, gas supply, ventilating and air conditioning engineering from Shenyang

This work is licensed under a Creative Commons Attribution-NonCommercial-NoDerivatives 4.0 License. For more information, see https://creativecommons.org/licenses/by-nc-nd/4.0/

This article has been accepted for publication in IEEE Access. This is the author's version which has not been fully edited and content may change prior to final publication. Citation information: DOI 10.1109/ACCESS.2023.3336706

Jianzhu University, Shenyang, China, in 2008. Her current research interests include building environment, building energy efficiency, and green building technologies.

CHUNYONG LUO received the Ph.D. degree in geotechnical engineering from Zhejiang University, Zhejiang, China, in 2004. Her current research interests include environmental geotechnical engineering, remediation of contaminated soils, and groundwater contamination migration.

WEIDONG PAN received the M.S. degree in measuring and testing technologies and instruments from Kunming University of Science and Technology, Kunming, China, in 2005. His current research interests include image processing, defect detecting, and image mosaiking.

This work is licensed under a Creative Commons Attribution-NonCommercial-NoDerivatives 4.0 License. For more information, see https://creativecommons.org/licenses/by-nc-nd/4.0/